Active Dynamic Flow Control Studies on Rotor Blades

W.Geissler, M.Trenker, H.Sobieczky

Deutsches Zentrum für Luft- und Raumfahrt e.V., Institut für Strömungsmechanik,

Bunsenstr. 10, D-37073 Göttingen, Germany

Abstract:

Higher Harmonic Control (HHC) and Individual Blade Control (IBC) technologies have reduced noise and vibration levels of rotors considerably. Further improvements are expected with **on-blade** devices, i.e. the rotor blade is active only along a limited spanwise section of high aerodynamic efficiency.
On both advancing and retreating sides of the rotor disc local supersonic areas terminated by shock waves play a dominant role with respect to separation (dynamic stall) and buffet (moving shock) problems.
The present paper deals with new design methodologies to deform blade sections dynamically. The objective of airfoil deformation is to avoid strong shock waves which are responsible for shock induced separation (dynamic stall) on the retreating blade and which are the origin of high speed impulsive noise levels on the advancing blade.
A combination of different software components available at DLR Institute of Fluid Mechanics, i.e. Geometry Generation Tools and 2D-Time Accurate Navier-Stokes Codes have already shown their strong potential for the development of dynamic flow control devices. This system will be used intensively in the present study and systematically applied to separation and shock control problems.

1. Introduction

The design of helicopter rotor airfoils is a matter of compromise:

-Take care of transonic effects on the advancing side of the rotor disc

-Try to reduce or at least shift unsteady separation (dynamic stall) on the retreating side of the disc.

Fig. 1 shows the main flow problems on a helicopter in forward flight. With increasing flight speed the main rotor encounters transonic flow with shock waves on the outer part of the blade where strength as well as position of the shocks are dependent on time i.e. on the azimuth angle.
On the retreating side the incidence of the blade has to be increased to balance the overall lift of the rotor. Simultaneously with the transonic flow on the advancing side reversed flow and flow separation occurs on the retreating side a phenomenon called dynamic stall. The latter flow feature has frequently been described in the literature [1],[2].
A rigid airfoil design can not take care of all problems in an optimal way. Several investigators have therefore proposed passive as well as active control devices to favorably influence unsteady separation (dynamic stall):

- suction and blowing devices on the airfoil upper surface (both steady and dynamic), [3],
- leading edge flap, [4]
- trailing edge flap, [5], etc.

In recent years a different type of control device has been proposed: The dynamically deforming airfoil.
This type of device seems to have large potential with respect to dynamic stall control without the disadvantage of i.e. the static flap device which is not very useful on the advancing side of the cycle.
Different concepts have been tried with considerable benefit:
Fig. 2 shows two of recently applied devices which are the "nose-drooping" concept frequently investigated at DLR, [6] and the DDLE (Dynamically Deforming Leading Edge) concept, [7] investigated at NASA, [8].
Both concepts have the main feature to either shift (nose-droop) or reduce (DDLE) the local curvature at the airfoil leading edge and do this dynamically, that is time dependent. In the case of the DDLE-concept a wind tunnel model has been realized which has a flexible leading edge surface made from carbon fiber. The flexible structure is dynamically deformed by means of a pull/ push rod operating inside the model. By means of this device the curvature of the NACA 0012 airfoil model could be reduced considerably and leading edge separation was shifted to higher incidences or in optimal cases could be completely avoided.
Numerical investigations, [9] show at least qualitative comparison with the experimental data.
To realize the nose-droop concept on a wind tunnel model is a much more difficult task. The proposal given in Fig. 2 has frequently been calculated numerically. It has been shown, [10] that the dynamic stall vortex can be reduced considerably in strength (see Fig.3) resulting in improved force and moment hysteresis loops.
However the realization of this device which covers more than 25% of the airfoil surface with rather high deflection angles can not be realized nowadays on either a wind tun-

Paper presented at the RTO AVT Symposium on "Active Control Technology for Enhanced Performance Operational Capabilities of Military Aircraft, Land Vehicles and Sea Vehicles", held in Braunschweig, Germany, 8-11 May 2000, and published in RTO MP-051.

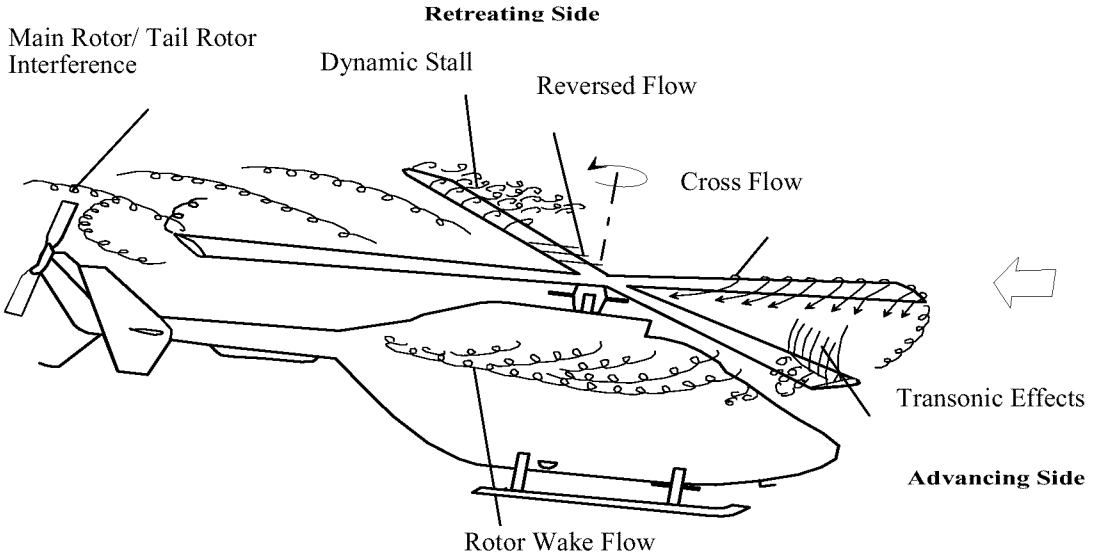

Fig. 1: Main Flow Problems on Helicopter in Forward Flight

nel model nor on the real rotor blade.

With the development of new actuator design based on pieco-electric devices it is now possible to move parts of the airfoil dynamically as rigid structures. In [11] it has been shown that corresponding actuators are able to oscillate a trailing edge flap with sufficient deflection angles and frequencies. The same actuator system will be used in future wind tunnel tests to operate a sealed leading edge flap under realistic aerodynamic loads (German project AROSYS, joint project between DLR, ECD, Daimler-Chrysler Research Lab).

In the present paper it will be shown first that this leading edge flap concept is already of considerable benefit with respect to dynamic stall control. However the advancing side of the blade has to be taken into account as well. New design methodologies are now available at DLR to take also care of the transonic flow conditions, [12]. By means

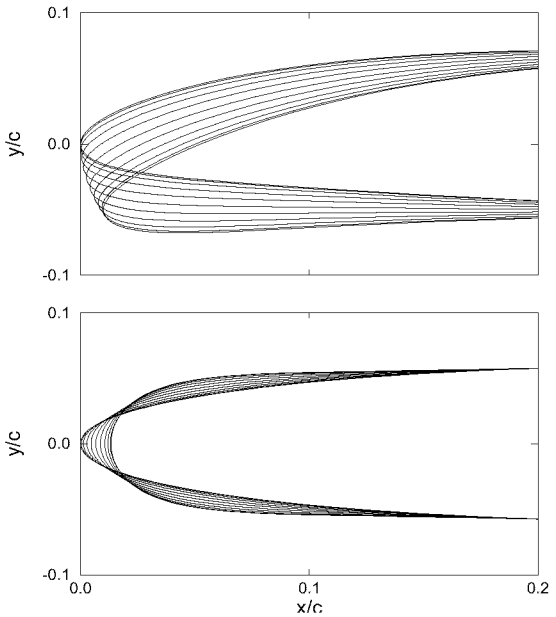

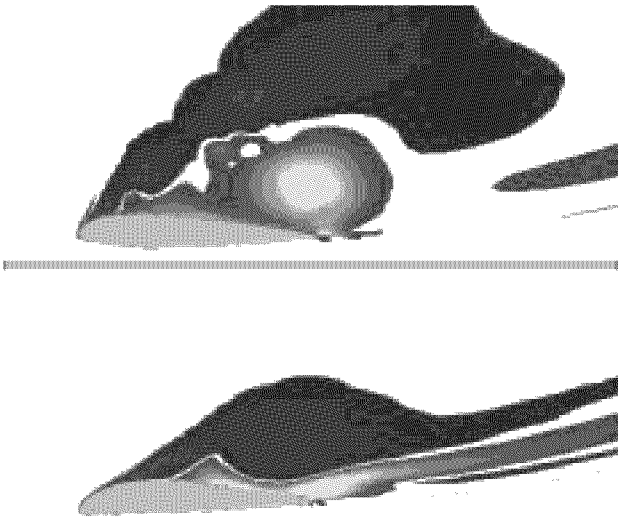

Fig. 2 ((Left): Nose-Droop (Upper), Dynamically Deforming Leading Edge (Lower), Fig. 3 (Right): Dynamic Stall Vortex reduction by a Nose-Drooping Device

of shock free design methods based on the "fictitious gas" concept, [13] a new airfoil will be developed which has optimal flow conditions at the transonic design point and which is in addition equipped with a nose-drooping device to favorably represent the retreating side of the rotor disc.

2. Realization of airfoil deformation on wind tunnel models.

Within the german RACT (Rotor Active Control) project, [11] it has been demonstrated that a system of pieco-electric actuators inside the wind tunnel model was able to operate a trailing edge flap under realistic aerodynamic loadings. Flap deflections of 3^o amplitude and frequencies of up to 5/ref of the fundamental model frequency of 7Hz was reached over the complete Mach number range $0.3 < M < 0.75$.

A similar model is under construction to operate on a leading edge flap with 10% chord and a maximum flap deflection of 10^o. Fig.4 shows the model arrangement with the oscillating part of the leading edge.

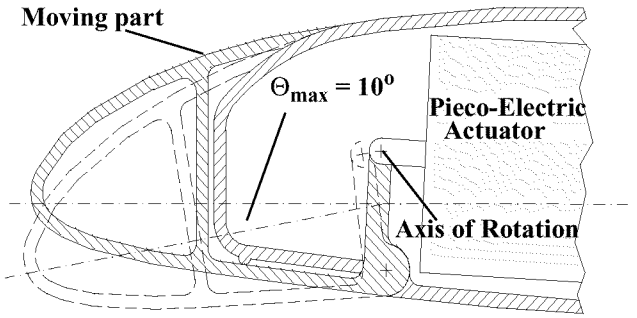

Fig.4: Structural Realization of Nose-Droop Design

The deforming leading edge surface is defined and discretized in space and time by means of the Geometry Generator Tools of DLR, [14]. With the pre-calculation of the deforming surface the calculation of the structured and deforming grid around the airfoil can start. The flow solver used for the flow calculations is a time-accurate Navier-Stokes code, [15] based on the Reynolds averaged Navier-Stokes equations (RANS). The grid around the sealed and deforming leading edge flap is allowed to deform with respect to time. This feature of the code is necessary to take into account dynamically deforming parts of the airfoil surface. Comparisons of numerical results show good correspondences with experimental data from the RACT-tests, [5] where a sealed trailing edge flap was oscillating. The present configuration is not an optimal device but it is a feasible construction for wind tunnel tests. In the following it will be shown that this device has already considerable benefits with respect to improvement of dynamic stall characteristics.

3. Selection of test case for aerodynamic design of airfoil with combined pitching and lead/lag-motions.

The numerical code, [15] has been extended to combine both pitching motion and lead/lag motion of the airfoil. The latter is simulating the Mach number variation. A characteristic set of parameters has been defined for numerical calculations:

a) Pitching motion about the quarter chord axis
$\alpha=10^o+10^o \sin(\omega^*T)$

b) Lead/Lag motion (Mach number variation)
$M=0.50-0.23 \sin(\omega^*T)$

c) Parameters:
$\omega^*=0.3$ (referred to chord)
$Re=2*10^6$

Maximum time-window for nose-drooping the airfoil: between 10^o upstroke and 10^o downstroke with the maximum deflection ($\Theta_{max} = 10^o$, Fig.4) at the maximum incidence of $\alpha=20^o$.

Numerical features of the Navier-Stoke code:
- Structured grid with 361x71 grid points
- Spalart-Allmaras turbulence model
- 20 000 time-steps/period
- calculation of two to three periods.

The calculations have been carried out fully turbulent. In future investigations the transition options included in the code, [16] will also be taken into account to better match the experimental data.

4. Force, moment and pressures on helicopter airfoil with nose-droop.

Fig. 5 shows lift-, drag- and pitching moment hysteresis loops for the

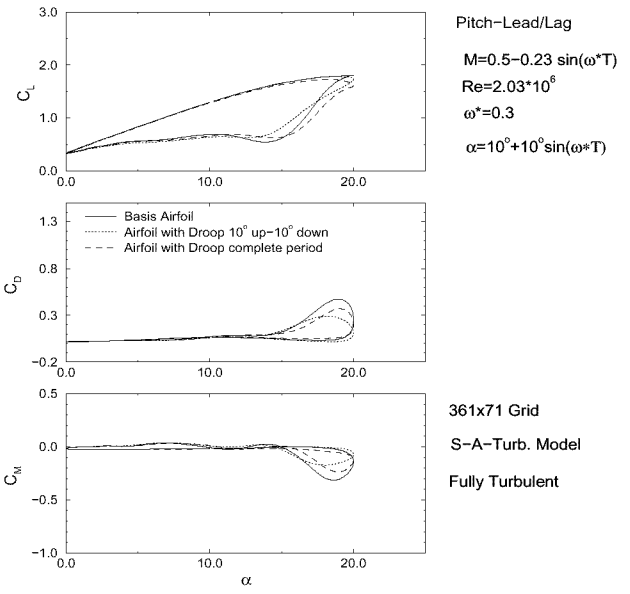

Fig.5: Force and Moment Distributions

- rigid airfoil
- drooping airfoil with droop between 10^o up and 10^o down
- drooping airfoil with droop over complete cycle

The main results of the plots are:
- the droop about the limited time window shows the same maximum lift compared to the rigid airfoil
- the maximum drag and minimum pitching moment are both reduced considerably in the drooping case compared to the rigid airfoil.

The benefit of dynamic stall i.e. the lift increase is retained in the drooping case, the drag and moment loops show strong improvements.

Figs. 6a (rigid airfoil) and 6b (drooping airfoil) show the corresponding pressure and skin friction distributions during the high incidence variation (retreating blade) of the airfoil. The pressure distributions in Fig.6a show a second maximum on the upper surface indicating the effect of the dynamic stall vortex moving along the airfoil upper surface into the wake. In the drooping case (Fig.6b) the effect of the dynamic stall vortex is not completely suppressed but its influence has been considerably reduced. Improvements can also be observed in the skin friction distributions (lower plots in Figs. 6a and 6b).

A more condensed presentation of the space and time dependent pressure distributions of both rigid and drooping airfoils are presented in the "mountain-plots" of Figs.7a (rigid) and 7b (drooping).

In Figs 7a and 7b the pressure is plotted versus the airfoil

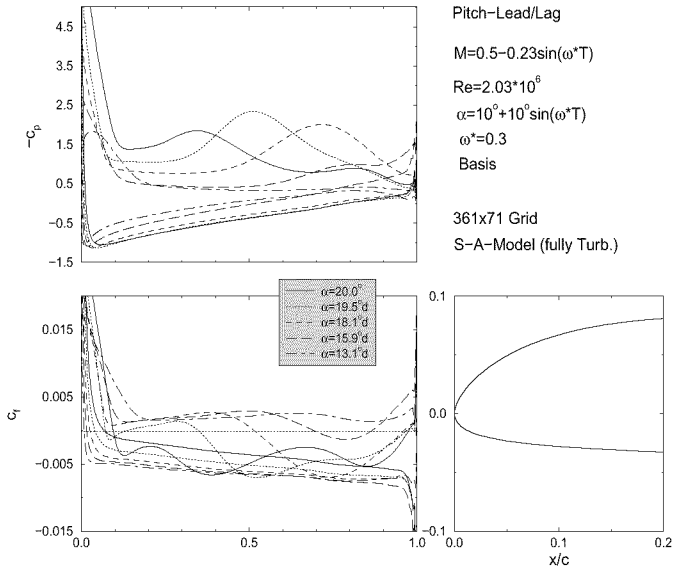

Fig. 6a: Pressure and skin friction on rigid airfoil

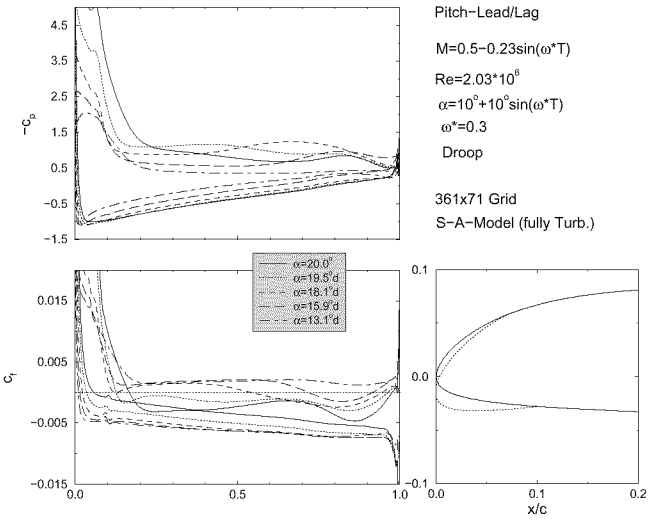

Fig. 6b: Pressure and skin friction on drooping airfoil

surface coordinate s/c from trailing edge lower to trailing edge upper side respectively and versus time with T as dimensionless time from start to end of one period of oscillation.

It can clearly be detected from Figs 7 that the strong pressure peak at the high incidence region

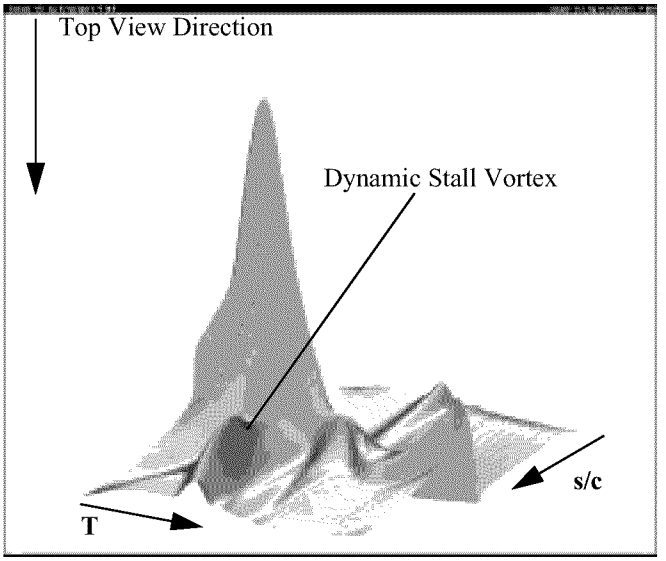

Fig.7a: Pressure Mountain versus Time and Space, rigid airfoil.

of the oscillation has been reduced remarkably by the airfoil drooping. The reason is that the adverse pressure gradient is smoothed, the dynamic stall vortex although still present has been reduced in strength as well. In both figures 7 a top view direction is indicated which is shown

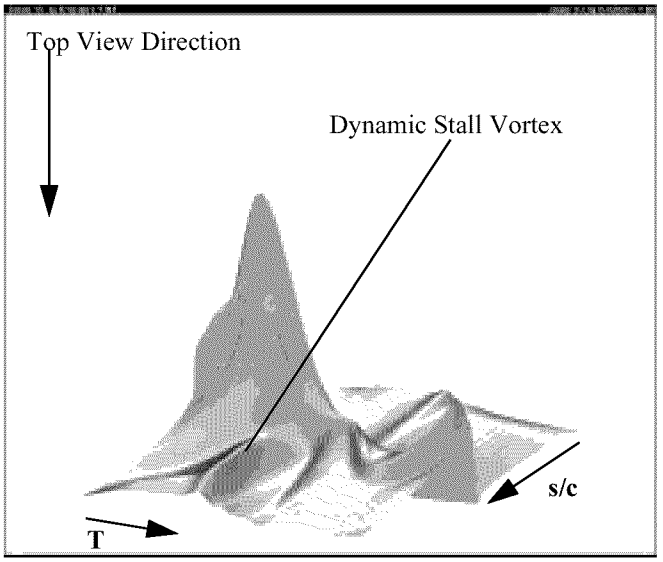

Fig.7b: Pressure Mountain versus Time and Space, drooping airfoil.

in Figs.8.
The effect of the dynamic stall vortex on the upper surface pressure distribution can again be detected in these plots. The strength of the vortex is reduced in the drooping case of Fig.8b. It can already be seen in Figs. 7 but it is more clearly indicated in Figs.8 that in the high Mach number regime of the oscillatory cycle a shock wave is developing both in space and time. It is obvious that this effect has not been influenced by the nose-drooping device. In the following the design methodology will be extended to improve also the aerodynamic behavior of the flow in the transonic region corresponding to the advancing side of the rotating blade.

5. Design methodology for advancing part of rotor cycle (transonic area).

Up to now the helicopter airfoil has been modified at the leading edge for dynamically drooping the airfoil. It has been demonstrated that considerable benefit is achieved by the drooping device although the drooping has not been optimized with respect to stall control but has been designed in order to match the construction constraints for a planned wind tunnel model.
In the following it will be shown how the airfoil can be reshaped by means of the Geometry Generation Tool, [14] based on shock free design methodology. The drooping device as described above will also be kept with the new airfoil design. It will be shown that improvements are achieved on both advancing **and** retreating sides of the cycle.

6. Application of Fictitious Gas Concept for shock free design of airfoils.

The Fictitious Gas Concept (FGC) and its application to transonic design of shock free aerodynamic configurations was proposed and extensively investigated by Sobieczky and Seebass, [13]. The main objective of FGC is to develop shock free airfoils at the design conditions. FGC has recently been applied with numerical calculation procedures based on the Euler equations, [17].
For the following investigations the present time-accurate Navier-Stokes code has to be modified to account for FGC:

- the supersonic region filled with the fictitious gas of everywhere subsonic speed is different to inviscid flow now a **closed region** closing up inside the boundary layer

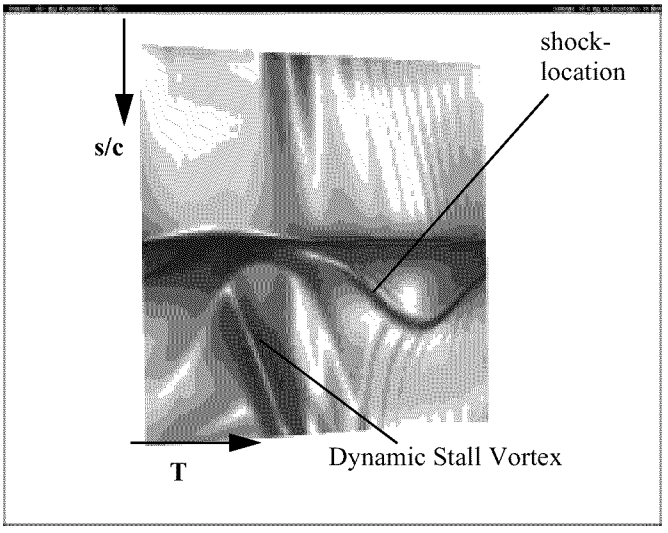

Fig. 8a: Top view of pressure distribution of Fig.7a

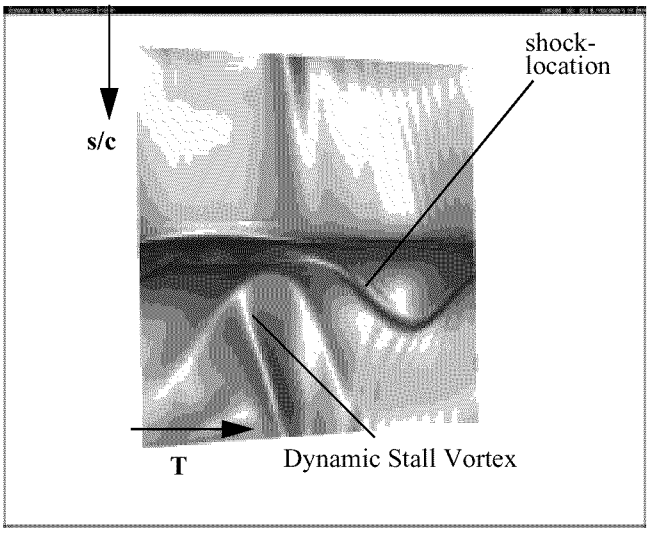

Fig. 8b: Top view of pressure distribution of Fig.7b

- the pressure and density along the sonic line limiting the FG-area is no longer constant inside the boundary layer. The dependency of p and ρ on turbulent viscosity is not known by analytical expressions but is dependent on the turbulence model chosen. Hence this dependency can only be determined numerically
-if the flow is time dependent, the development of the supersonic region with respect to time has also to be represented, if the NS-solver is running in the FG mode.

The main steps to be done to modify the NS-code are characterized as follows:
- switch between perfect gas and fictitious gas inside the supersonic region by changing the pressure density relation, [17],
- represent smooth transition from perfect gas in the outer flow field to subsonic FG-region inside the originally supersonic area, with M=1 along FG-boundary,
- calculate converged result including the FG-region.
Fig. 9 shows shematically a result of this calculation: The FG-region comes out to be smooth in the former shock wave region. But the result is fictitious. Additional steps have to be carried out to get a shock free solution:

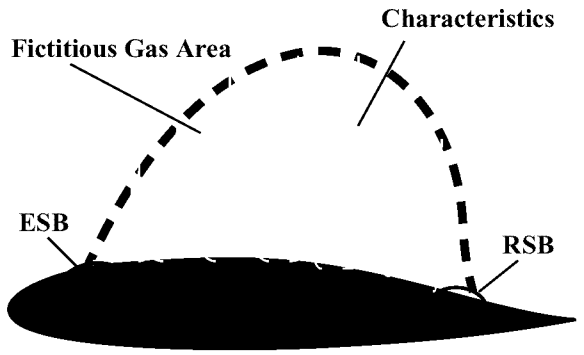

Fig.9: Fictitious Gas Concept (FGC)

a) The FG-region is filled again with perfect gas
b) inside the FG-area the method of characteristics is applied
c) the surface of the airfoil covered by FG is no longer a streamline
d) the airfoil upper surface is modified to be a streamline again
e) a numerical calculation in the perfect gas mode is done for the modified airfoil.

In order to keep the modification of the airfoil small a minor **local** modification of the airfoil surface using bumps at both upstream and downstream position of the intersection of the sonic line with the airfoil can be used.
Fig.9 shows these modifications as ESB (Expansion Shoulder Bump) and RSB (Recompression Shoulder Bump). This bump modification however will not be completely shock free.
Due to the fact that a viscous flow solver is used, the FG-region is not touching the airfoil surface but is sitting on top of the boundary layer (not indicated in Fig.9). To correctly modify the airfoil surface the boundary layer displacement surface is taken into account for the surface modification.

7. Results of approximately shock free airfoil (advancing side) and nose-drooping airfoil (retreating side).

For the selected incidence and Mach number variation selected in 3) the complete design procedure has been carried out step by step:
As start configuration a new airfoil section is developed by means of the Geometry Generation Tool.
This new airfoil which has the same thickness distribution as the original one is now modified to a shock free design using the different steps described in the previous section for the application of FGC. For the shock free design a design point with M=0.73 and $\alpha=1.1^{o}$ has been selected. The result is of course only shock free in the design point. It remains to be demonstrated how this airfoil behaves under unsteady conditions with varying α and M.
Fig.10 shows the results of the different design steps up to this point.
The upper left figure indicates the new airfoil design without pre-drooping and s-shape camber line. The NS-calculation in the selected design point determines a strong shock wave at about mid chord of the airfoil. The calculation in the FG-mode leads to Mach number contours
as shown in the lower left plot of Fig.10 with the FG-region indicated. Applying the method of characteristics inside the FG-region the airfoil upper surface has to be modified to be again stream surface as is shown on the lower right plot. The NS-calculation in the perfect gas mode about the modified airfoil finally gives an almost shock free pressure distribution as indicated in the upper right figure.
So far the design of the rigid airfoil section with shock free characteristics at the design point has been demonstrated.
The next step is to modify the leading edge of this new airfoil by a dynamic nose-droop device as has been described in the previous sections and which is shown in Fig.4 to be suitable for realization on a real wind tunnel model with in situ actuator systems.
The design steps for the drooping device are identical as described before and have again been determined by means of the Geometry Generator Tools of DLR.
The final proof of the total system including dynamic nose-drooping has been calculated by the NS-code. In the following some typical results will show the benefit of the design procedures with respect to both transonic and separating flow domains.

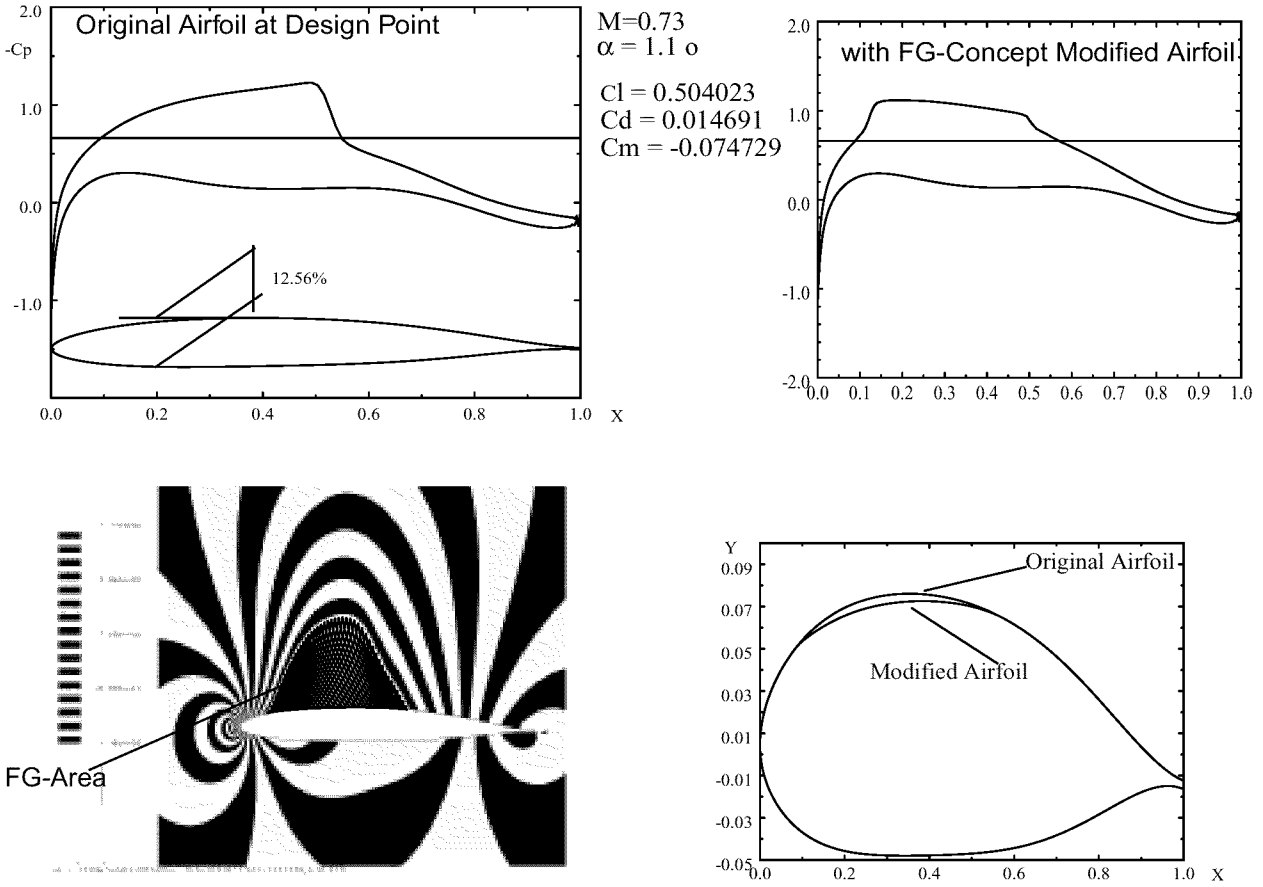

Fig10:Airfoil Shape Modification by Means of Fictitious Gas- (FG-) Concept

Fig.11 shows the final airfoil shape including the nose-drooping area at the leading edge with 10% chord flap area. With combined pitching and lead/lag motions as described in section 3) and with the additional nose-drooping now in the time-window between 12.1° up and 12.1° down (the incidence variation has slightly been increased to: $\alpha=12.1^{o}+11^{o}\sin(\omega*T)$) the Mach contours in Fig.12 and the following sequences of figures show improvements first of the shock free design compared to the basis airfoil: The airfoil is not only shock free at the design point but shows also improvements i.e. shock strength reductions within a larger time window during the oscillation cycle. This can be seen in Fig.12 at the second half of the cycle where the area of reduced shock strength is clearly visible. The first half of the cycle shows that the separation area has been shifted toward the trailing edge such that the leading edge part with the moving slat still produces aerodynamic loads.

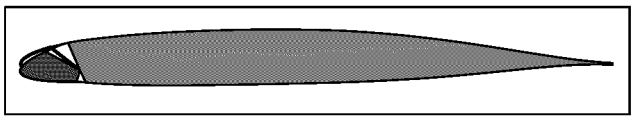

Fig.11 New airfoil design with nose-droop, A1510

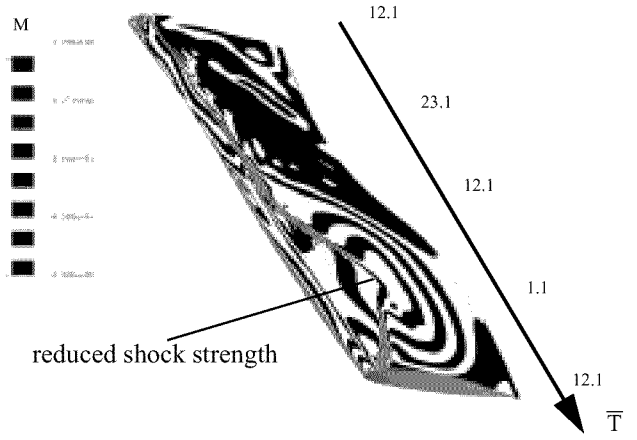

Fig.12 Mach-contours in time and space of final NS-calculation

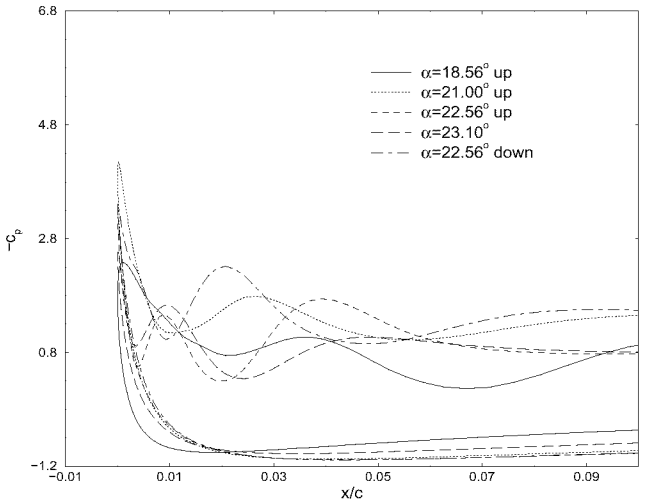

Fig. 13a: Pressure distributions in the leading edge region of the basis airfoil (separated flow)

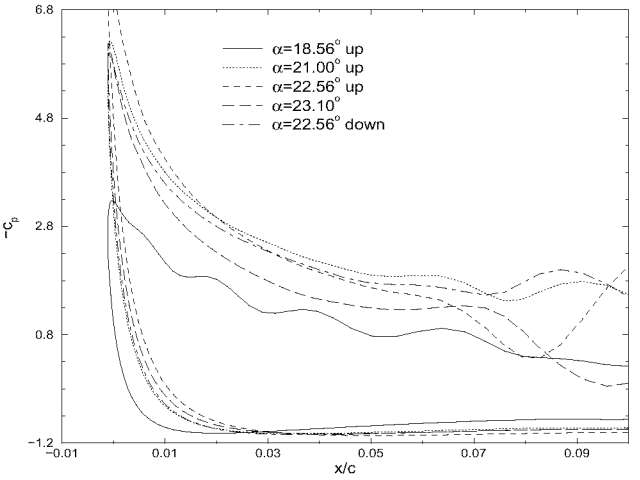

Fig.13b: Pressure distributions in the leading edge region of the modified airfoil with nose-droop (separated flow)

Figs. 13a and 13b show pressure distributions during the high incidence part of the oscillation loop where the formation of a dynamic stall vortex and its shedding takes place. Fig. 13a shows severe effects of the dynamic stall vortex indicated by a secondary pressure peak developing along the airfoil upper surface. Compared to the corresponding curves of Fig.13b the loading on the first 10% of the airfoil is considerably higher. The effect of a dynamic stall vortex is shifted further downstream. Similar improvements can also be detected from the skin friction distributions (not shown). In the basic airfoil case reversed flow occurs up to the very leading edge. The drooping airfoil has extended regions in time and space where the flow does not separate.

Figs.14 finally show the corresponding pressure distributions during the transonic flow regime (advancing side). Fig.14a includes again the pressure distributions of the basis airfoil. A rather strong shock wave can be detected which develops in time (α-variation). The modified airfoil (Fig.14b) shows shock free pressure distributions at the design point, i.e. at $\alpha=1.1^{o}$. But the pressure curves in the vicinity of the design point show also strong improvements with respect to shock strength development. Again the skin friction distributions (not shown) show improvements with respect to the fact that shock induced separation does not occur.

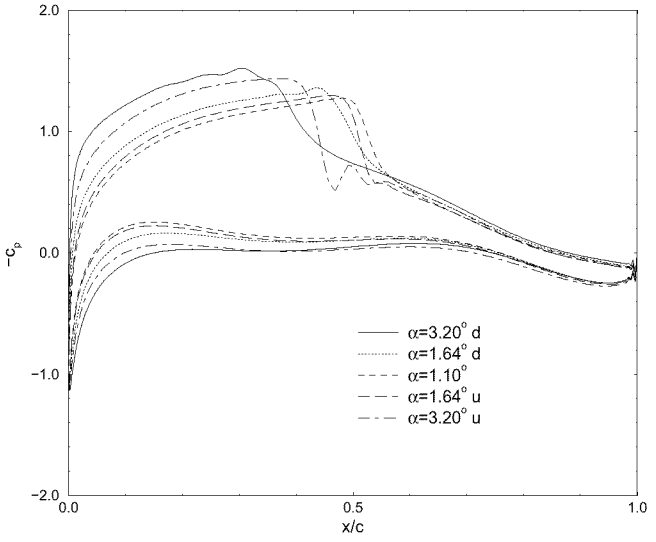

Fig.14a: Pressure distributions in the leading edge region of Basis airfoil (transonic Flow)

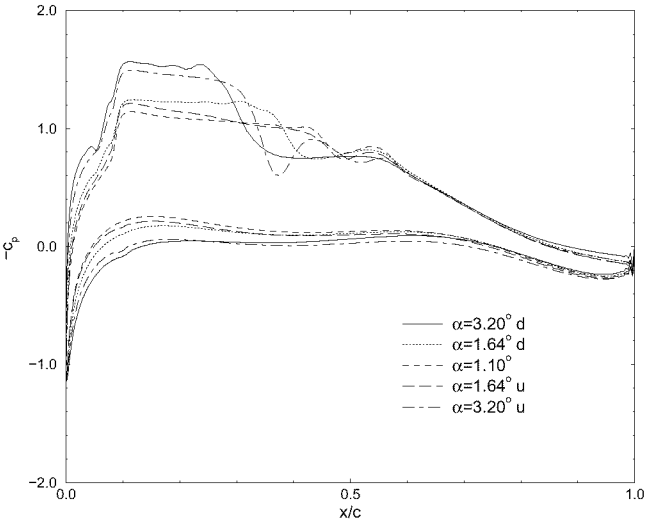

Fig.14b: Pressure distributions in the leading edge region of the modified airfoil (transonic flow)

8. Conclusions

New developments of design tools and their combination with suitable flow solvers based on the Reynolds averaged Navier-Stokes equations have demonstrated their capabilities to study new design concepts with dynamically deforming leading or trailing edge deformations. New actuator designs based on pieco-electric principles have shown their capabilities to 1) be small and light enough to be implemented inside a wind tunnel model or a rotor blade and 2) have shown to operate the flap with the necessary deflection angles and frequencies.

The present study goes one step further: A new airfoil shape is designed which is modified in such a way that it is shock free within a selected design point. This new airfoil is then equipped with a nose-drooping device similar to the one which will be realized on a wind tunnel model with embedded actuator system.

The results which have been found by numerical investigations show considerable benefits in the transonic area of the cycle (advancing side) as well as in the region of the development of dynamic stall (retreating side) of the cycle. The modified airfoil shows remarkable reductions of the shock strength not only at the design point but also within a time window adjacent to the design point. On the retreating side dynamic stall onset is shifted to later time (higher incidences) by means of the drooping device. The aerodynamic loading on the drooping area is kept over almost the complete cycle.

In the future the complete design procedure has to be improved and simplified towards an optimized design. It has to be investigated if a closed loop design procedure is feasible.

9. References

[1] McCroskey,W.J.," Some Current Research in Unsteady Fluid Dynamic - The 1976 Freeman Scholar Lecture", Journal of Fluid Engineering, Vol.99,March 1977, pp.8-38.

[2] Carr,L.W. "Progress in Analysis and Prediction of Dynamic Stall", Journal of Aircraft, Vol.25,No.1,January 1988, pp.6-17.

[3] Allrefai,M., Acharya,M. ,"Controlled Leading Edge Suction for the Management of Unsteady Separation over Pitching Airfoils", AIAA Paper 95-2188,June 1995.

[4] Carr,L.W., Chandrasekhara,M.S., Wilder,M.C., Noonan,K.W.,"The Effect of Compressibility on Suppression of Dynamic Stall Using a Slotted Airfoil", AIAA 36th Aerospace Sciences Meeting & Exhibit,
January 12-15,1998,Reno, NV.

[5] Geissler,W.Sobieczky,H.Vollmers,H.,"Numerical Study of the Unsteady Flow on a Pitching Airfoil with Oscillating Flap"
24th European Rotorcraft Forum, 15-17th September,1998, Marseilles, France, Paper AE09

[6] Geißler,W., Sobieczky,H.,"Dynamic Stall Control by Variable Airfoil Camber",
AGARD 75th Fluid Dynamics Panel Meeting and Symposium on Aerodynamics and Aeroacoustics of Rotorcraft.October,10-14,1994,Berlin,Germany,pp.6.1-6.10.

[7] Chandrasekhara,M.S., Wilder,M.C., Carr,L.W., "Unsteady Stall Control Using Dynamically Deforming Airfoils", AIAA-Paper 97-2236, June 23-25, 1997, Atlanta,GA.

[8] Chandrasekhara,M.S., Wilder,M.C., Carr,L.W., "Unsteady Stall Control Using Dynamically Deforming Airfoils", AIAA Journal,Vol.36,No.10,October 1998.

[9] Geissler,W., Carr,L.W., Chandrasekhara,M.S.,
Wilder,M.C., Sobieczky,H.,"Compressible Dynamic Stall Calculations Incorporating Transition Modeling For Variable Geometry Airfoils", 36th AIAA Aerospace Meeting and Exhibit, January, 12-15, 1998,
Reno Hilton, Reno, NV.

[10] Geißler, W.,Sobieczky, H.,"Unsteady Flow Control on Rotor Airfoil", AIAA 13th Applied Aerodynamics Conference, 19.-22. June, 1995, San Diego, CA, USA, pp. 1-9.

[11] Schimke,D.,Jänker,P.,Wendt,V.,Junker,B.,"Wind Tunnel Evaluation of a Full Scale Pieco-Electric Flap Control Unit", 24th European Rotorcraft Forum,15-17 Sept.,1998,Marseilles,France.

[12] Sobieczky,H., Geissler,W.,"Active Flow Control Based on Transonic Design Concepts",17th AIAA Applied Aerodynamics Conference,
June 28-July 1,1999, Norfolk, VA.

[13] Sobieczky,H., Seebass,A.R., "Supercritical Airfoil and Wing Design", Ann.Rev.Fluid Mech.16,pp.337-363 (1984).

[14] Sobieczky,H.,"Geometry Generator for Aerodynamic Design", CISM Course and Lectures No. 366, 'New Design Concepts for High Speed Air Transport', Springer, Wien,New York (1997), pp. 137-158.

[15] Geissler,W.,"Instationäres Navier-Stokes Verfahren für beschleunigt bewegte Profile mit Ablösung (Unsteady Navier-Stokes Code for Accelerated Moving Airfoils Including Separation)" in german, DLR-FB 92-03 (1992).

[16] Geissler,W., Chandrasekhara,M.S.,
Platzer,M., Carr,L.W.,"The Effect Of Transition Modeling On The Prediction Of Compressible Deep Dynamic Stall", 7th Asian Congress of Fluid Mechanics,
Dec. 8-12, 1997, Chennai (Madras), India.

[17] Li,P., Sobieczky,H.,"Computations of Fictitious Gas Flow with Euler equations", Acta Mechanica (1994),[Suppl] 4:251-257,Spriger Verlag 1994.

This page has been deliberately left blank

Page intentionnellement blanche